Video Article

Gene Regulation and Targeted Therapy in Gastric Cancer Peritoneal Metastasis: Radiological Findings from Dual Energy CT and PET/CT

Bowen Shi[1], Huimin Lin[1], Miao Zhang[2], Wei Lu[3], Ying Qu[4], Huan Zhang[1]

[1]Department of Radiology, Ruijin Hospital, Shanghai Jiao Tong University School of Medicine

[2]Department of Nuclear Medicine, Ruijin Hospital, Shanghai Jiao Tong University School of Medicine

[3]GE Healthcare China

[4]Department of Surgery, Cedars-Sinai Medical Center

Correspondence to: Ying Qu at Ying.Qu@cshs.org, Huan Zhang at huanzhangy@126.com

URL: https://www.jove.com/video/56526
DOI: doi:10.3791/56526

Keywords: Medicine, Issue 131, Gastric cancer, peritoneal metastasis, animal model, gene regulation, targeted therapy, imaging, dual energy CT, PET/CT

Date Published: 1/22/2018

Citation: Shi, B., Lin, H., Zhang, M., Lu, W., Qu, Y., Zhang, H. Gene Regulation and Targeted Therapy in Gastric Cancer Peritoneal Metastasis: Radiological Findings from Dual Energy CT and PET/CT. *J. Vis. Exp.* (131), e56526, doi:10.3791/56526 (2018).

Abstract

Gastric cancer remains fourth in cancer incidence worldwide with a five-year survival of only 20%-30%. Peritoneal metastasis is the most frequent type of metastasis that accompanies unresectable gastric cancer and is a definitive determinant of prognosis. Preventing and controlling the development of peritoneal metastasis could play a role in helping to prolong the survival of gastric cancer patients. A non-invasive and efficient imaging technique will help us to identify the invasion and metastasis process of peritoneal metastasis and to monitor the changes in tumor nodules in response to treatments. This will enable us to obtain an accurate description of the development process and molecular mechanisms of gastric cancer. We have recently described experiment using dual energy CT (DECT) and positron emission tomography/computed tomography (PET/CT) platforms for the detection and monitoring of gastric tumor metastasis in nude mice models. We have shown that weekly continuous monitoring with DECT and PET/CT can identify dynamic changes in peritoneal metastasis. The sFRP1-overexpression in gastric cancer mice models showed positive radiological performance, a higher FDG uptake and increasing enhancement, and the SUV_{max} (standardized uptake value) of nodules demonstrated an obvious alteration trend in response to targeted therapy of TGF-β1 inhibitor. In this article, we described the detailed non-invasive imaging procedures to conduct more complex research on gastric cancer peritoneal metastasis using animal models and provided representative imaging results. The use of non-invasive imaging techniques should enable us to better understand the mechanisms of tumorigenesis, monitor tumor growth, and evaluate the effect of therapeutic interventions for gastric cancer.

Video Link

The video component of this article can be found at https://www.jove.com/video/56526/

Introduction

Gastric cancer (GC) remains the fourth most common malignancy and the second-leading cause of cancer mortality worldwide[1]. Although the accuracy in diagnosis and treatment of gastric cancer has been greatly improved, peritoneal metastasis is the most key point of gastric cancer prognosis or recurrence and is a definitive determinant of postoperative death[2]. It is generally accepted that peritoneal dissemination is a life-threatening mode of metastasis, wherein the disease becomes uncontrollable and the prognosis of the patient is poor once peritoneal dissemination is established. Therefore, the detection and therapeutic effect evaluation of gastric cancer peritoneal metastasis is crucial for clinical practice.

The increasing incidence and mortality of gastric cancer had spurred researchers to identify its molecular mechanisms. The high expression of genes such as secreted frizzled-related protein 1 (sFRP1) might lead to activation of the signal pathway in the early stages of gastric cancer, promoting the process of tumor growth, proliferation, differentiation, and apoptosis[3,4,5,6,7]. sFRP1-overexpression cells showed an increase in the expression of TGFβ, its downstream targets, and TGFβ-mediated EMT[8]. Previous studies have demonstrated that the TGF-β1 level is correlated with peritoneal metastasis and the TNM stages of gastric cancer. We have described the changes in cancer cell proliferation regulated by sFRP1 overexpression and TGF-β1 inhibition, and established animal models for peritoneal metastasis to show the performance of tumor imaging under the effects of gene regulation.

Animal models for gastric cancer are indispensable tools for researching tumor development and experimenting with various therapeutic strategies without having to sacrifice animals. Animal models have proven useful in studying the formation mechanisms of tumors and cells of origin, determining the presence of cancer stem cells, and examining various novel therapeutic strategies. Therefore, a real-time non-invasive technique can provide an accurate description of the development of gastric tumors and tumor response to treatments, which can identify the development of peritoneal metastasis nodules in nude mice and monitor the changes of a tumor in response to various experimental and therapeutic interventions.

Currently, multi-detector CT (MDCT) plays an important role in the TNM staging of gastric cancers and is useful for predicting tumor resectability preoperatively[9]. However, radiological studies of patients with histologically proven gastric carcinoma have mainly been based on morphology. DECT imaging extends the parameters to reflect functional information by providing monochromatic images and may be helpful for improving the N staging accuracy for gastric cancers. Furthermore, this technique will enable the acquisition of material-decomposition images, which may be useful to differentiate between differentiated and undifferentiated gastric carcinoma, and between metastatic and non-metastatic lymph nodes[10]. With the introduction of DECT, the functional imaging aspect of CT has also been added to clinical applications, contributing to evaluations of therapeutic efficacy and predicting patient prognoses[11,12,13]. PET/CT is a useful imaging technique for the detection and staging of gastric cancer and can evaluate the recurrence of the tumor effectively[14]. Tumor cell proliferation and angiogenesis were both considered to be necessary in the development of a detectable tumor[15], tumor nodules showed a positive performance with higher SUV_{max} on PET/CT. Based on their preference for aerobic glycolysis, ^{18}F-FDG, a glucose analog, has been exploited as a promising tracer in the diagnosis of malignancies, combined with PET/CT[16]. This method relies on the rapid glucose consumption of tumor tissue and has broad clinical applications, including assisting in the detection, staging, and evaluation of the prognosis of tumors, as well as monitoring the tumors' response to therapy[17,18]. As non-invasive methods, DECT and PET/CT have been utilized to diagnose malignant tumors and to assess tumor response to various therapies.

Our group has been using this non-invasive imaging method with DECT and PET/CT scanners to detect and monitor the process of tumor growth and metastasis in living mice[19]. We explored imaging findings induced by the sFRP1-overexpression in gastric cancer cells *in vivo* using nude mice, with DECT and PET/CT, and described the changes of the SUV_{max} value following targeted therapy by the TGF-β1 inhibitor to confirm the development of tumor nodules in the peritoneum after gene induction, and also studied the changes in tumor nodules in response to experimental treatments. In this paper, we present detailed procedures for modeling gastric tumor peritoneal metastasis in mice, and its detection and monitoring with DECT and PET/CT.

Protocol

This work was performed in strict accordance with the standards established by the Guidelines for the Care and Use of Laboratory Animals of Shanghai Jiao Tong University and was approved by the laboratory Animal Ethics Committee of Ruijin Hospital.

1. Gastric Cancer Peritoneal Metastasis Animal Model

1. Divide a moderately differentiated SGC-7901 human gastric cancer cell line into an SGC-7901/sFRP1 group and an SGC-7901/vector group. Culture the two groups of cells separately in RPMI 1640 supplemented with 10% fetal bovine serum, 100 units/mL streptomycin, and 100 μg/mL penicillin at 37 °C in a humidified atmosphere with 5% CO_2.
2. Use 4-6 week-old female athymic BALB/c nude mice with body weights of 25 to 30 g. Place animals under specific pathogen-free conditions in an animal facility.
3. Divide mice randomly into the sFPR1 overexpression group and the sFPR1 empty loading group.
   NOTE: Each group had ten nude mice; twenty mice were randomly divided into TGF-β1 treatment group and TGF-β1 control group, with up to 5 nude mice per animal cage.
4. Establish the sFPR1-overexpression peritoneal metastasis xenograft models group by administering 150 μL (2 x 10^6 cells/mL) suspensions of SGC-7901/sFRP1 cells via the abdominal cavity; SGC-7901/vector cells are administered to establish the empty loading group.
   NOTE: Use a hemocytometer counting method to determine the concentration of cells[20].
5. **Establish the peritoneal metastasis xenograft models group by administering 150 μL (2 x 10^6 cells/mL) suspensions of SGC-7901 cells via the abdominal cavity. Administer the target therapy of TGF-β1 inhibitor SB431542 after a period of two weeks of growth by intraperitoneal injection at a dose of 100 μL/10 g of body weight every other day to mice in the treatment group.**
   1. Administer normal saline at the same dose to mice in the control group.
6. Perform the DECT and PET/CT scanning 1 day before treatment and 1 day, 7 days, 14 days, and 21 days after treatment.

2. DECT for Peritoneal Metastasis Animal Model

NOTE: The animal imaging experiment was achieved on the dual energy CT scanner (see **Table of Materials**). We created the related DECT imaging protocol according to the previous studies.

1. **Setup for DECT imaging protocol**
   1. On the imaging console computer, select the "protocol management" icon to enter the next interface, then click the "protocol management" option to view the protocol management screen.
   2. In the 'User protocol' interface, select the abdomen area to enter the abdomen protocols list.
   3. Click the blank space in the protocol lists and select the "New" button to type the name of a new protocol: "Animal DECT Scan". Press the "Enter" key on the keyboard and select the "Scout" button in the pop-up window, click "OK" to setup the scout series (the first series).
   4. Select the "XY" mode for 'Anatomical Reference Point' and the "head-first supine position" for 'Patient Orientation'. Click on the "auto transfer" option and select the workstation location where the image series will be uploaded. Name "Scout phase" in Series Description.
   5. In the 'View Edit' screen, make sure the relevant scan parameters are set as the following: "Start location" and "End Location" options are set at "S50" and "I50" respectively, "KV" at "100", "mA" at "80", "90°" for "Lateral scout position", "0°" for "AP scout position", and the "scout WW/WL" at "400/40".
   6. Next, create the second series for non-enhanced scanning. Click "Create New Series", in the pop-up window to select the "Axial" and "Create After" icons.
   7. Name the series as "-C phase" in the Series Description and turn "Show localizer" on. In the Scan type interface, select the "helical" scan type and 0.5 s for "Rotation Time", click "Thick Speed" option to set the parameters (Detector Coverage at 40 mm, Helical

Thickness at 0.625 mm, Pitch and speed at 0.516:1/20.62, Rotation Time at 0.5 s) in the pop-up window, Interval at 0.625 mm, Gantry Tit at 0, SFOV select Small Body, kV at 100, click "mA" then type 600 for Manual mA.

8. Click the "Recon Parameters" icon and open the "Recon Option" pop-up window. Select "Plus" in Recon Mode; click the "Slice" icon to select "ss50 slice 50%" mode in the 'ASiR Setup screen'. Set the remaining parameters as follows: DFOV at 25 cm, R/L and A/P Center at 0 cm, Recon type select "Stnd", Matrix Size at 512.
9. Create the third scan series for enhanced scanning by repeating the step 2.1.8, name it as "+C QC phase" and turn "Show localizer" on; the first group is the setup of arterial phase series.
10. In the 'Scan type' interface, click on "GSI (Gemstone Spectral Imaging)" and select "helical" scan type, select the protocol "GSI-52" in the 'Abdomen GSI Preset Selection' window. Set start Location and end Location according to the non-enhanced scanning.
    1. Click the "Recon Parameters" icon and open the "Recon Option" pop-up window. In Recon Mode, select "Plus" and in 'GSI option' click "QC"; the remaining parameters are the same as in step 2.1.8.
11. Click the "R2" icon and select "YES" in the "Recon enabled" tab. Select "Thickness" at 0.625 and type 0.625 for "Interval". Open the "Recon Option" pop-up window, in Recon Mode select "Plus"; in GSI options, click "Mono" and set the keV to 70 keV; in the ASiR Setup window, select the "GS40 40%" mode for the GSI ASiR setup. The remaining parameters are set with step 2.1.8. Name this step as "+C 70keV phase".
12. Click the "R3" icon and select "YES" in the "Recon enabled" tab. Set "Thickness" at 1.25 and type 0.625 for "Interval". Open the "Recon Option" pop-up window, in Recon Mode select "Plus" and "IQ enhanced"; in the GSI options, click "Mono", set the keV to 70 keV and click "GSI Data File"; ensure the GSI ASiR setup is in accordance with step 13. The remaining parameters are set as in step 2.1.8. Name this as "+C Mono phase".
13. Click "Add group" to create two scan groups to represent the portal phase and the delay phase, respectively. Make sure that the "Start Location" and "End Location" ranges of each scan phase are consistent and the remaining parameters are the same as the arterial phase. Type the delay time in "Preparation Group": the first group (arterial phase) at 0 s, the second group (portal phase) at 8 s, and the third group (delay phase) at 16 s.
14. Click the "Accept" option to save the protocol after all the settings are done.

2. **DECT imaging process**
    1. Select the nude mice randomly from the treatment and control groups before each scan. Place the selected animals in new cages and mark them separately.
    2. Fast the mice for 4 h with water but without food or bedding.
    3. Remove the experimental mice from the animal experiment center 1 h before the scan, and make sure the mice are placed in a new warm environment until the scan begins.
    4. Anesthetize all the experimental mice with an intraperitoneal injection of 2.5% pentobarbital sodium (1.0 mL/kg body weight) before DECT scan imaging, and confirm the depth of anesthesia by the toe pinch reflex. Use ointment on the eyes to prevent dryness while under anesthesia.
       NOTE: Ensure that the head of each nude mouse is in the lower position when injecting the drugs, thus reducing damage to the internal organs. Pay attention to the injection site and the depth of injection. Place the tip of the syringe at a 45° angle to the inside of the right/left lower abdomen, and ensure that the needle depth is such that injection into the bowel and other organs is avoided.
    5. Click the "New Patient" icon, input the basic information about the mouse including its patient ID and name. In the 'User protocol', click the "abdomen protocol" and select the "Animal DECT Scan" protocol to enter the operation interface.
    6. Once anesthesia is induced, move each mouse onto an animal fixture platform in the supine position, and fix its tail with tape to make sure it does not bend. Sterilize the tail with alcohol for subsequent contrast agent injection into the tail-vein.
    7. Move the CT scan bed so that the external positioning line laser is over the lower abdomen of the animal. Click the "reset" button when the positioning is completed.
       NOTE: The placement of external positioning lines over the lower abdomen of the animal ensures that the animals are located as far as possible on the outside of the machine for easy contrast agent administration into the tail vein.
    8. Click the "Confirm" icon and follow the flashing order of the buttons on the keyboard to complete the scout scanning. Select the "next series" icon after the scout scanning is completed, and enter the interface for non-enhanced scanning.
    9. In the right screen, set the "Start Location" and "End Location" on the scout views to define the scan range. Maintain the same range in 'Lateral scout' and 'AP scout' and cover the entire body volume of the animal.
    10. Click the "Confirm" icon and follow the flashing order of the buttons on the keyboard to complete the scout scanning.
    11. Inject each mouse with iopamidol at a dosage of 0.2 mL/100 g through the tail vein.
        NOTE: We chose to administer the contrast medium manually and keep the injection rate as stable as possible. It is most conducive to capture the early enhancement of the tumor during imaging.
    12. Click "next series" to perform enhanced scanning. Set "Start Location" and "End Location" as per the non-enhanced scan. Click the "confirm" icon and follow the flashing order of the buttons on the keyboard to complete the dynamic enhanced scans, includingarterial phase, portal phase, and delayed phase.
        NOTE: Click the "Confirm" icon immediately to start scanning after the contrast agent is injected. This is essential and crucial for enhanced scanning to ensure the best image of the arterial phase is captured. However, some delay time after clicking the "confirm" icon can ensure that the experimental staff has withdrawn safely from the scanning room.
    13. Click "End exam" to exit the scanning interface after the scanning is complete; the image series will be automatically uploaded to the workstation.
    14. Place the animal into an empty cage after completion of the scan with all mice, and observe them until they have regained consciousness.Do not leave an animal unattended until it has regained sufficient consciousness to maintain sternal recumbency. Then transfer the mice into a clean animal room.

3. **Post DECT imaging analysis**
    1. Locate the mice series on the DECT workstationinterface (see **Table of Materials**) and select the "+C Mono phase" series lists. Open "GSI Volume Viewer" and select "GSI VV General" protocol from the 'GSI Protocol Manager' interface.

2. Click the "View Type" active annotation at the upper-left corner of the image viewports and select "coronal" orientation from the drop-down menu.
3. For one image viewport, click the "Volume 1" active annotation at the upper-left corner and select "Mono" volumes from the drop-down menu. Similarly, in another image viewport, select "Iodine (Water)" volumes. Click and hold the left mouse button, drag the image from "Iodine (Water)" viewport to "Mono" and check the "mix the views" box to get the color fused images.
4. Click and drag from the center of the "Image Scroll" icon to observe images. Save the images which show positive results as color fused images.

3. PET/CT for Peritoneal Metastasis Animal Model

NOTE: See the table of materials for the PET/CT imager used. We created the related PET/CT imaging protocol according to this article[21].

1. **Setup Micro-PET/CT Imaging Protocol**
   1. For a whole-body CT scan, set current at 500 μA, voltage at 80 kV, exposure time at 200 ms, and 240 steps for 240° rotation. For X-ray detector, select resolution at "low system magnification" with 78 mm axial imaging field and single bed mode. Use the "Common Cone-Beam Reconstruction" method and select the "real time reconstruction" option, so that the host PC can connect with the dedicated real time reconstruction computer (Cobra) to initiate the task.
   2. For PET acquisition, in the "acquire by time" option set "fixed scan time" to 600 s (10 min). Set "study isotope" to F-18 and "energy level" to 350-650 keV.
   3. To produce the PET Histogram, set the "dynamic frame" as "black" to process data as one frame for the entire duration to achieve static scan. Set histogram type to "3D" and select the "no scatter correction" option.
   4. For PET reconstruction, reconstruct images using an OSEM3D algorithm followed by MAP or Fast MAP[22] provided by PET/CT workstationsoftware (see **Table of Materials**).

2. **Preparation before PET/CT imaging**
   1. Fast the mice which have undergone DECT experiments for 4 h and transfer the mice to new animal cages 30 min before imaging.
   2. Weigh the mice and record their weight.
   3. Follow the institute's safety procedures to acquire and carry the package containing radioactive materials (RAM). Use a protective shield to carry the ^{18}F-FDG (5 mCi), and measure the radioactivity of the total ^{18}F-FDG with a dose calibrator.
   4. Dilute the ^{18}F-FDG with normal saline to the appropriate radioactivity of mice injection.
      NOTE: The diluted activity of ^{18}F-FDG should be available at 100-200 μCi/100 μL for each mouse.
      1. Draw 200 μL ^{18}F-FDG solution into a 1 mL syringe. Measure the radioactivity of the whole syringe with a dose calibrator and record the ^{18}F-FDG preparation time.
   5. Inject each mouse with 200 μL ^{18}F-FDG solution via the tail intravenous injection route and record the ^{18}F-FDG injection time. After the injection of all mice, measure the residual radioactivity of the syringe with the dose calibrator immediately and record the time that the measurements were taken after completion of the injection.
   6. Calculate the injected ^{18}F-FDG activity for each mouse by the following formula: Injected activity (μCi) = activity in syringe before injection - activity in syringe after injection.

3. **PET/CT Imaging Process**
   1. Put the animal into an anesthesia induction chamber; anesthetize mouse using inhaled 3% Isoflurane in oxygen after the completion of ^{18}F-FDG injection.
      NOTE: Follow all animal welfare guidelines appropriate for operation; keep the mice warm by using the heating pad. Use ointment on eyes to prevent dryness while under anesthesia.
   2. Once anesthesia is induced, move the mouse onto the micro-CT scanning bed while maintaining continuous anesthesia and warming. Position the head of the mouse within a cone face mask that continuously delivers Isoflurane (2%) in oxygen at a flow rate of 2 L/min. Place the mouse in supine position to ensure the posture is consistent with that in DECT scans.
   3. Move the animal to the entrance of the PET/CT scanner, click the "laser" icon from the toolbar viewer, and use the touchpad control interface to move the bed so that the abdomen of the mouse is located at the center of the PET and CT field-of-view (FOV) during scanning. In the "Laser Align" window, select "first scan type" as "CT scan", and "PET acquisition included in workflow" as the option.
   4. Open the "Scout View" window and acquire a scout view X-ray radiograph. Adjust the position of the animal bed so that the center field of view of the CT is located at the center of the mouse body.
   5. Select the protocol established previously (in step 3.1). Input the number of mice to be imaged (successively) in the pop-up window and click the "Setup" option, then enter the weight. Then click the "Setup" option again and follow the pop-up window instructions to complete the setup.
   6. Click the "Start Workflow" icon to start scanning.
   7. Evaluate the quality of the acquired CT and PET images after all the scans are completed. Transfer the data through the network to the post imaging analysis for further study.
      NOTE: Adjust the window width and window level of the image to ensure that the contrast of the organs is displayed properly. Check the resolution of the organs in the images to confirm the imaging quality.
   8. Remove the animal from the imager and immediately euthanize by cervical dislocation. Use the imaging system for the next animal successively.

4. **Post PET/CT imaging analysis**
   1. Open the PET/CT workstation software, import the CT and PET image series data into the software. In the "Registration" window, click the "General analysis" option to register CT and PET images together, and choose the "Sky" model under the "Review" window to show a perfect alignment between CT and PET images.

2. Identify the peritoneal nodules with references provided by the co-registered images in the "Region of Interest (ROI) Quantification" window.
3. In the "Region of Interest (ROI) Quantification" window, draw ROI with tools over the fused images, edit the size and shape of ROI, record the SUV_{max} value, then output and save the selected merged images.

Representative Results

DECT and PET/CT scanning were performed on nude mice after two weeks of cell line injections. GSI images yielded excellent results for displaying subcutaneous metastasis beyond the contour of the abdomen for the sFRP1 overexpression group, and metastasis with peripheral enhancement was confirmed by color-scale image (**Figure 1a-c**). PET/CT images depicted focally abnormal FDG uptake of metastasis, including in the peritoneal and subcutaneous metastases (**Figure 1d**). The peritoneal metastasis and large subcutaneous metastasis shown on the DECT and PET/CT images were further illustrated by gross specimen and histological section (**Figure 1e-f**). Compared with the positive expression group, there were no visible lesions, obvious abnormal enhancements, or high FDG uptake in the abdominal cavity in the sFRP1 empty loading group from DECT and PET/CT images (**Figure 2a-b**). Though the images of the gross specimen and histological results confirmed the successful implantation for this group (**Figure 2c-d**).

The intervention treatment of TGF-β1 inhibitor and placebowere performed on nude mice after two weeks of cell line injections, and DECT and PET-CT scanning were performed on nude mice after two weeks of treatment. To confirm the process of the formation of peritoneal metastasis nodules in mice from the initiation of target therapy, follow-up DECT and PET/CT scans were performed. Non-invasive imaging scans were performed to assess the effect of TGF-β1 targeted treatment. The images for the mice in the TGF-β1 treatment group depicted obvious enhancement and focal abnormal FDG uptake of metastases in the coronal fused images of DECT and PET/CT (**Figure 3a-b**). Gross specimens illustrated only 8 nodules of peritoneal metastases (**Figure 3c**) with diffused distribution in the abdominal cavity. Quantitatively, **Figure 3** showed moderate peripheral enhancement on DECT and reduced FDG uptake, with an SUV_{max} close to 0.83. On the other hand, mice in the control group that were given normal saline also showed visible lesions and focally abnormal uptake of metastases in the coronal fused images of DECT and PET/CT (**Figure 4a-b**). Gross specimens illustrated 22 nodules of peritoneal metastases (**Figure 4c**), and the local metastasis nodules were adherent to the abdominal cavity. The SUVmax values in the tumors were not changed (at 1.26) for mice in the control group that were given normal saline.

It is noteworthy that sometimes the intestinal tract will cause FDG mild ingestion and the bright region in the images will produce false positive results.The heart and bladder will also gather a lot of FDG, which may show as a bright spot in the images.It is necessary to avoid the relevant level images to determine the real FDG uptake area of tumor.

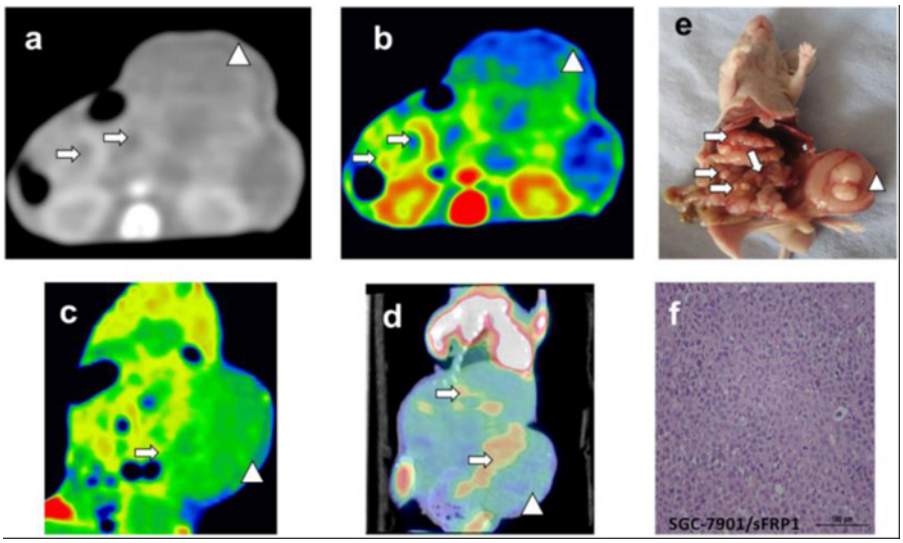

Figure 1: Tomogram of sFRP1 overexpression group peritoneal metastasis model from DECT, PET/CT and corresponding HE staining. (**a-c**) GSI monochromatic images in portal phase: (**a**) transverse monochromatic image, (**b**) transverse color-fused image, (**c**) coronal color-scale image; (**d**) coronal fused images of PET/CT, (**e**) gross specimen, (**f**) histological section. Arrows indicate the peritoneal metastatic nodules, while arrow heads indicate the subcutaneous metastasis. **Figure 1f** is the pathological staining result of a tumor nodule; the image shows the morphology and distribution of tumor cells; Scale bar = 100 μm. This figure has been modified from reference[19]. Please click here to view a larger version of this figure.

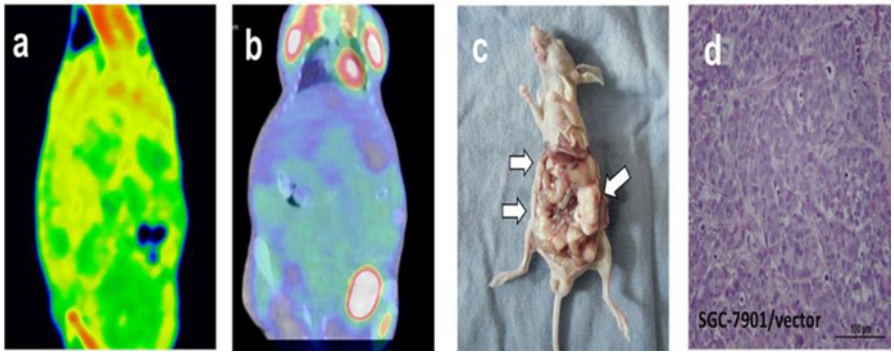

Figure 2: Tomogram of sFRP1 empty loading group peritoneal metastasis model from DECT, PET/CT and histological analysis. (**a**) GSI color-scale fused images obtained in portal phase, (**b**) fused PET/CT image, (**c**) gross specimen, and (**d**) histological section. No visible lesion, obvious abnormal enhancement or high FDG uptake was shown in the abdominal cavity. (**c**) and (**d**) confirmed the successful implantation. The arrow heads in **Figure 2c** pointed out the peritoneal metastatic nodules caused by the SGC-7901/vector cell lines. The heart and bladder showed obvious FDG elevation in **Figure 2b**. **Figure 2d** is the pathological staining result of a tumor nodule; the image shows the morphology and distribution of tumor cells; Scale bar = 100 μm. This figure has been modified from reference[19]. Please click here to view a larger version of this figure.

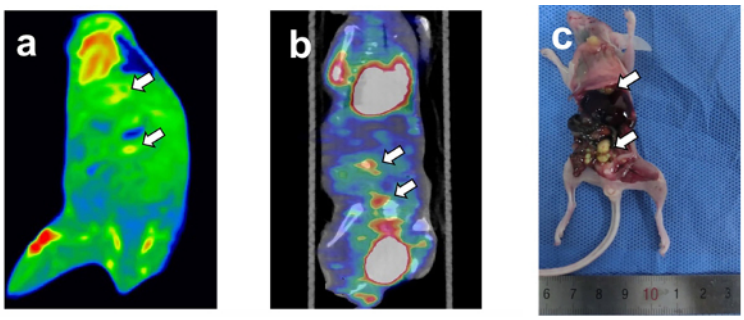

Figure 3: Tomogram of TGF-β1 treatment group peritoneal metastasis model by DECT and PET/CT and corresponding gross specimen. (**a**) the coronal fused image of DECT, (**b**) the fused images of PET/CT. (**c**) gross specimen. The heart and bladder showing obvious FDG elevation in the **Figure 3b**. Gross specimen illustrated 8 nodules of peritoneal metastases. Arrows pointed out the metastatic nodules corresponding to the radiographic finding. Please click here to view a larger version of this figure.

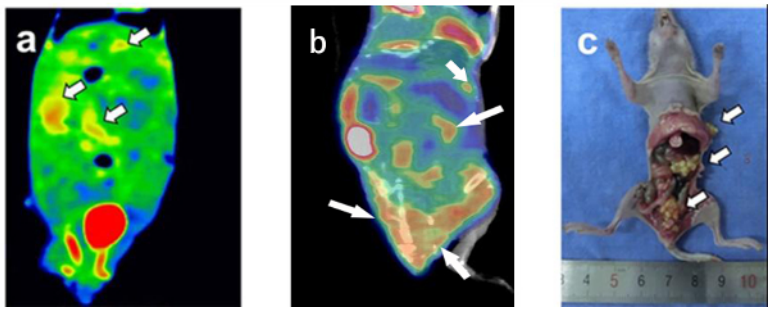

Figure 4: Tomogram of TGF-β1 control group peritoneal metastasis model by DECT and PET/CT and corresponding gross specimen. (**a**) The coronal fused image of DECT, (**b**) the fused images of PET/CT, and (**c**) gross specimen. Gross specimen illustrated 22 nodules of peritoneal metastases. Arrows pointed out the metastatic nodules corresponding to the radiographic finding. Please click here to view a larger version of this figure.

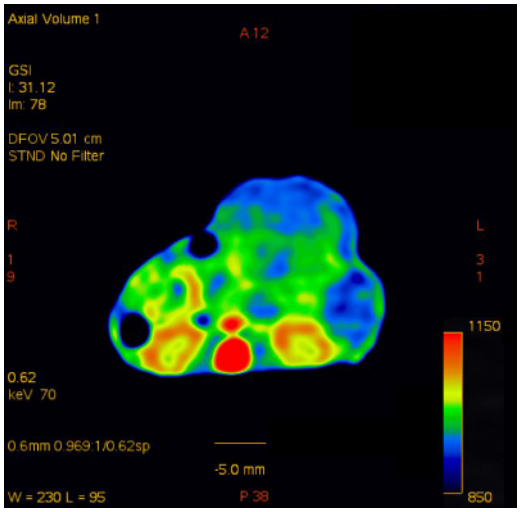

Supplementary Figure 1: Sample transverse color-fused image. Please click here to view a larger version of this figure.

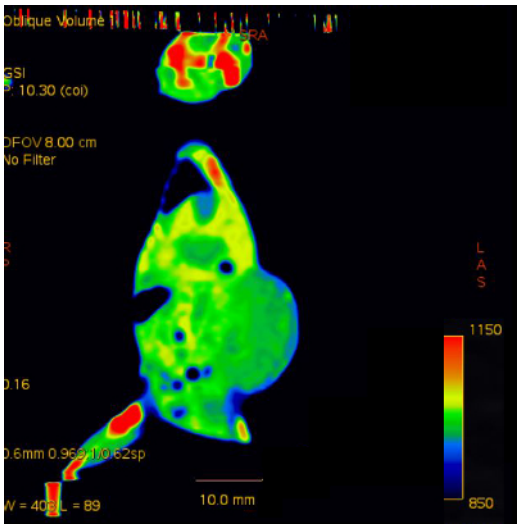

Supplementary Figure 2: Sample coronal color-fused image. Please click here to view a larger version of this figure.

Discussion

Animal models have been used widely in the study of molecular mechanisms underlying gastric cancer, and to experiment with various therapeutic strategies[23,24,25]. In this study, we have described a detailed protocol for gastric cancer peritoneal metastasis nude mice modeling, using DECT and PET/CT to image gastric tumors for identifying tumor cell proliferation in real-time, and monitoring peritoneal metastasis and responses to therapeutic interventions in gastric cancer animal models. This method could enable researchers who are involved in studying the molecular mechanisms of gastric cancer, or experiments imaging tumors, to establish more integrated and precise plans. In addition, we described the use of DECT and PET/CT devices that can serve as platforms for discovering tumor imaging performance with gene regulation and target therapy. Therefore, the method may be used by scientists to understand and explore the biological processes of cancer recurrence and progression. We have demonstrated that the non-invasive imaging modality could detect increased tumorigenesis by the overexpression of genes with positive results on DECT and PET/CT. Simultaneously, peritoneal metastasis after therapeutic intervention with targeted inhibitor showed negative FDG uptake performance on PET/CT. The SUVmax of tumor nodules presented a downward trend by extension of the treatment cycle.

In our study, we used the change in FDG uptake as an assessment indicator of therapeutic effects for peritoneal metastasis. Great effort has been put forth to show that FDG uptake is associated with tumor aggressiveness[26]. Progressive gastric carcinomas, represented by the depth of invasion, lymphatic permeation, vascular invasion, and tumor size, show higher FDG uptake[27]. In terms of quantitative evaluation, studies suggested that the SUV_{max} has a positive correlation with proliferation in various malignancies[15,28]. Our results demonstrated that compared with the control group, sFRP1 overexpression positively induced visibly larger nodules with significantly increasing enhancement and higher FDG uptake in peritoneal tumors, as was evidenced in **Figure 1**. In addition, the SUVmax showed an obvious alteration trend in the target treated groups, in contrast to no change in the control group. These results were demonstrated in **Figure 3** with a decreased FDG uptake, with an SUVmax close to 0.83 for the treatment group, as opposed to an unchanged SUVmax value of close to 1.26 for mice in the control group that were given normal saline (**Figure 4**). Our results indicated that non-invasive imaging techniques, such as DECT and PET/CT, provide the possibility of using image technology to assess information at the molecular level in tumor cells and demonstrated the validity of combining the applications of DECT and PET/CT to provide a viable, reproducible, and non-invasive imaging strategy to monitor tumor nodules induced by

gene modulation for gastric cancer research. Since the FDG uptake is associated with tumor aggressiveness[26], the utilization of PET/CT imaging to assess the degree of tumor invasion and treatment is feasible.

In our previous studies, we have found that the injection time and method could influence the imaging results of DECT scanning. As the circulation chanages quickly in mice, and the enhancement of peritoneal metastasis mainly occurs in the arterial phase, the peritoneal metastases nodules may not be displayed completely if the scan begins significantly later than the injection time. The nude mice should be placed in a warm and clean environment after the examination, letting the mice rest for 12 h before PET/CT imaging to avoid the effects on the nodules' uptake of ^{18}F-FDG in PET/CT imaging with excessive residual contrast agent in the body. Attention should be paid to the injection time and activity in the preparation and injection of FDG. The optimal activity concentration of ^{18}F-FDG for PET/CT was about 100-200μCi/100μL for each injection. Too high of a concentration could increase the burden of circulatory system and result in the death of mice, while too low of a concentration might interfere with tumor uptake imaging. So, it is critical to ensure the efficiency and accuracy of the ^{18}F-FDG configuration. Make sure that the PET/CT imaging position of nude mice is consistent with that of the DECT imaging to facilitate the matching of tumor images.

There are several limitations to our study. The limited resolution of DECT may contribute to the negative performance for visibility as some peritoneal tumors may exhibit insufficiently increasing size. It has been known that PET/CT has low specificity and a lack of anatomical localization, and the apoptosis and necrosis of tumor cells induced by chemotherapeutic drug interventions could influence the ^{18}F-FDG uptake[29,30]. In addition, the normal physiological activity in bowel loops and ^{18}F-FDG retention in ureters and bladder can contribute to false positives emerging in PET/CT images[31]. The process of peritoneal metastasis in nude mice models is difficult to detect and monitor, so the choice of appropriate time in therapeutic intervention and imaging experiments is particularly important. Therefore, the early diagnosis of small tumors is still a problem to be solved.

In conclusion, we have described a method that exploits DECT and PET/CT imaging technology for the accurate detection and evaluation of the efficacy of targeted therapy. Our results demonstrate that non-invasive imaging using the described protocols allows for the monitoring and evaluation of peritoneal metastasis progression using animal models. Applications of this method will be easily adapted for preclinical research aiming to discover gastric cancer peritoneal metastases, which may be useful to evaluate the disease diagnostic or therapeutic modalities.

Disclosures

The authors have no conflicts of interest to declare.

Acknowledgements

This work was supported by the NSFC (No. U1532107) and Shanghai Jiao Tong University Biomedical Engineering project (No. YG2014MS53). The authors would like to acknowledge Jianying Li and Yan Shen for their helpful comments and technical support efforts in developing the DECT and PET/CT imaging method.

References

1. Ferlay, J. *et al.* Cancer incidence and mortality worldwide: sources, methods and major patterns in GLOBOCAN 2012. *Int J Cancer.* **136** (5), E359-386 (2015).
2. Kobayashi, D., & Kodera, Y. Intraperitoneal chemotherapy for gastric cancer with peritoneal metastasis. *Gastric Cancer.* **20** (Suppl 1), 111-121 (2017).
3. Gu, W., Li, X., & Wang, J. miR-139 regulates the proliferation and invasion of hepatocellular carcinoma through the WNT/TCF-4 pathway. *Oncol Rep.* **31** (1), 397-404 (2014).
4. Sugai, T. *et al.* Molecular analysis of gastric differentiated-type intramucosal and submucosal cancers. *Int J Cancer.* **127** (11), 2500-2509 (2010).
5. Shi, Y., He, B., You, L., & Jablons, D. M. Roles of secreted frizzled-related proteins in cancer. *Acta Pharmacol Sin.* **28** (9), 1499-1504 (2007).
6. Amin, N., & Vincan, E. The Wnt signaling pathways and cell adhesion. *Front Biosci (Landmark Ed).* **17** 784-804 (2012).
7. Jones, S. E., & Jomary, C. Secreted Frizzled-related proteins: searching for relationships and patterns. *Bioessays.* **24** (9), 811-820 (2002).
8. Qu, Y. *et al.* High levels of secreted frizzled-related protein 1 correlate with poor prognosis and promote tumourigenesis in gastric cancer. *Eur J Cancer.* **49** (17), 3718-3728 (2013).
9. Pan, Z. *et al.* Determining gastric cancer resectability by dynamic MDCT. *Eur Radiol.* **20** (3), 613-620 (2010).
10. Pan, Z. *et al.* Gastric cancer staging with dual energy spectral CT imaging. *PLoS One.* **8** (2), e53651 (2013).
11. Kim, M. J., Hong, J. H., Park, E. S., & Byun, J. H. Gastric metastasis from primary lung adenocarcinoma mimicking primary gastric cancer. *World J Gastrointest Oncol.* **7** (3), 12-16 (2015).
12. Maeda, H., Kobayashi, M., & Sakamoto, J. Evaluation and treatment of malignant ascites secondary to gastric cancer. *World J Gastroenterol.* **21** (39), 10936-10947 (2015).
13. Bensinger, S. J., & Christofk, H. R. New aspects of the Warburg effect in cancer cell biology. *Semin Cell Dev Biol.* **23** (4), 352-361 (2012).
14. Smyth, E. *et al.* A prospective evaluation of the utility of 2-deoxy-2-[(18) F]fluoro-D-glucose positron emission tomography and computed tomography in staging locally advanced gastric cancer. *Cancer.* **118** (22), 5481-5488 (2012).
15. Oka, S., Uramoto, H., Shimokawa, H., Iwanami, T., & Tanaka, F. The expression of Ki-67, but not proliferating cell nuclear antigen, predicts poor disease free survival in patients with adenocarcinoma of the lung. *Anticancer Res.* **31** (12), 4277-4282 (2011).
16. Zhao, C. H., Bu, X. M., & Zhang, N. Hypermethylation and aberrant expression of Wnt antagonist secreted frizzled-related protein 1 in gastric cancer. *World J Gastroenterol.* **13** (15), 2214-2217 (2007).
17. Cheson, B. D. Role of functional imaging in the management of lymphoma. *J Clin Oncol.* **29** (14), 1844-1854 (2011).
18. Fuster, D. *et al.* Preoperative staging of large primary breast cancer with [18F]fluorodeoxyglucose positron emission tomography/computed tomography compared with conventional imaging procedures. *J Clin Oncol.* **26** (29), 4746-4751 (2008).

19. Lin, H. *et al.* Secreted frizzled-related protein 1 overexpression in gastric cancer: Relationship with radiological findings of dual-energy spectral CT and PET-CT. *Scientific Reports.* **7** 42020 (2017).
20. Cadena-Herrera, D. *et al.* Validation of three viable-cell counting methods: Manual, semi-automated, and automated. *Biotechnol Rep (Amst).* **7** 9-16 (2015).
21. Wang, X., Minze, L. J., & Shi, Z. Z. Functional imaging of brown fat in mice with 18F-FDG micro-PET/CT. *J Vis Exp.* (69) (2012).
22. Grootjans, W. *et al.* Performance of 3DOSEM and MAP algorithms for reconstructing low count SPECT acquisitions. *Z Med Phys.* **26** (4), 311-322 (2016).
23. Chang, H. R. *et al.* Improving gastric cancer preclinical studies using diverse in vitro and in vivo model systems. *BMC Cancer.* **16** 200 (2016).
24. Chang, H. R. *et al.* HNF4alpha is a therapeutic target that links AMPK to WNT signalling in early-stage gastric cancer. *Gut.* **65** (1), 19-32 (2016).
25. Zheng, H. C. *et al.* BTG1 expression correlates with pathogenesis, aggressive behaviors and prognosis of gastric cancer: a potential target for gene therapy. *Oncotarget.* **6** (23), 19685-19705 (2015).
26. Yamada, A., Oguchi, K., Fukushima, M., Imai, Y., & Kadoya, M. Evaluation of 2-deoxy-2-[18F]fluoro-D-glucose positron emission tomography in gastric carcinoma: relation to histological subtypes, depth of tumor invasion, and glucose transporter-1 expression. *Ann Nucl Med.* **20** (9), 597-604 (2006).
27. Hirose, Y. *et al.* Relationship between 2-deoxy-2-[(18)F]-fluoro-d-glucose uptake and clinicopathological factors in patients with diffuse large B-cell lymphoma. *Leuk Lymphoma.* **55** (3), 520-525 (2014).
28. Tchou, J. *et al.* Degree of tumor FDG uptake correlates with proliferation index in triple negative breast cancer. *Mol Imaging Biol.* **12** (6), 657-662 (2010).
29. Coleman, R. E. *et al.* Concurrent PET/CT with an integrated imaging system: intersociety dialogue from the Joint Working Group of the American College of Radiology, the Society of Nuclear Medicine, and the Society of Computed Body Tomography and Magnetic Resonance. *J Am Coll Radiol.* **2** (7), 568-584 (2005).
30. Brepoels, L. *et al.* Effect of corticosteroids on 18F-FDG uptake in tumor lesions after chemotherapy. *J Nucl Med.* **48** (3), 390-397 (2007).
31. Spaepen, K. *et al.* [(18)F]FDG PET monitoring of tumour response to chemotherapy: does [(18)F]FDG uptake correlate with the viable tumour cell fraction? *Eur J Nucl Med Mol Imaging.* **30** (5), 682-688 (2003).

